# PMPA: A PATCH-BASED MULTISCALE PRODUCTS ALGORITHM FOR IMAGE DENOISING

*Tao Dai, Chao-Bing Song, Ji-Ping Zhang, Shu-Tao Xia*

Graduate School at Shenzhen, Tsinghua University, Shenzhen, Guangdong, China
Tsinghua National Laboratory for Information Science and Technology, Beijing, China
Email:dait14@mails.tsinghua.edu.cn, scb12@mails.tsinghua.edu.cn, xiast@sz.tsinghua.edu.cn

## ABSTRACT

Patch-based algorithms for image denoising have been widely used in recent years. Most of patch-based methods just exploit patch redundancy in spatial or frequency domain without considering inter-scale dependencies. In this paper, we propose a novel patch-based multiscale products algorithm (PMPA) for image denoising. It is based on patch similarity in spatial domain and multiscale products in wavelet domain. PMPA is divided into two stages to process the smooth areas and non smooth areas (such as edges) individually. The first stage is in the wavelet domain, then a locally adaptive window-based denoising method (LAWML) based on multiscale products is applied to process those wavelet coefficients corresponding to the non smooth areas, then obtain one initial denoised image. The second stage is in the spatial domain, then a non local means algorithm is used to process those pixels in the smooth areas to obtain another initial denoised image. The final denoised image is obtained by a weighted averaging of all common pixels in both initial denoised images. Experiments show that the proposed algorithm can have competitive performance compared with the state-of-the-art patch-based denoising algorithms for most of images.

***Index Terms—*** Image denoising, nonlocal means, LAWML, wavelet, multiscale products

## 1. INTRODUCTION

Image denoising has been an important problem in the field of image processing for decades [1]. The aim of image denoising algorithms is to remove noise as much as possible while preserving important features. Wavelet-based techniques have been widely used and proven to be effective for image denoising due to the energy compaction property of wavelet transform [2, 3, 4, 5]. Generally, wavelet transform yields only a small number of large coefficients representing the important signal features (such as edges) and a large number of small coefficients representing the noise.

Several important denoising methods considering the intrascale or interscale dependencies in the wavelet domain have been proposed in the past years, which gain better performance than the traditional term-by-term wavelet denoising methods [6, 7, 8, 9]. Cai and Silverman proposed a thresholding strategy by taking account of the immediate neighbor coefficients [10]. Other famous strategies include bivariate distribution modes [11], Gaussian scale mixture (GSM) model [6], etc. The estimation results of these methods rely heavily on the accurateness of the model. In recent years, the most competitive denoising methods are mainly patch-based methods, such as nonlocal means (NL-means) [12], BM3D [13], LSSC [14] etc. In the patch-based methods, each patch is substituted by a weighted mean of the most similar patches found in the spatial domain. Typically, BM3D combines some tricks of clustering of noisy patches, shrinkage operation and DCT-based transform to achieve the state-of-the-art results [13].

In this paper, unlike BM3D, we propose a new patch-based multiscale products algorithm (PMPA) combining patch similarity in spatial domain and intra-and-interscale dependencies in frequency domain. PMPA is divided into two stages to obtain two initial denoised images. The first stage is in the wavelet domain, and we extend it to undecimated wavelet domain (UWT) and multiply the adjacent wavelet subbands obtaining the multiscale products to exploit the wavelet interscale dependencies. Besides, a locally adaptive window-based denoising method using maximum likelihood (LAWML) [15] is then applied to process those wavelet coefficients, corresponding to non smooth regions (such as edges in spatial domain), due to the simplicity and efficacy of LAWML. One advantage of multiscale products is that multiplying the adjacent wavelet subbands that can enhance edge structures while weakening noise. In the multiscale products, significant structures (such as edges) can be effectively distinguished from noise [8]. Hence, for each decomposition level of product subband, a threshold is calculated in the multiscale products. After that, a square window is used to perform traversal searches in the multiscale products so as to calculate the neighboring energy of products coefficients to identify significant features. After processing the wavelet coefficients by LAWML, we can obtain one initial denoised image by inversing wavelet transform. The second stage is in the spatial domain, then we use a NL-means method to process those smooth pixels, corresponding to smooth areas in the multiscale products, in the noisy image to exploit the patch redundancy directly. Likewise, we can obtain another initial denoised image by the NL-means method. Thus, the final denoised image is obtained by a weighted averaging of all common pixels in both initial denoised images.

## 2. RELATED WORKS

### 2.1. LAWML

Assume that an image $x$ is contaminated with additive white Gaussian noise (AWGN) with zero mean and variance $\sigma_n^2$, i.e.

$$y = x + n \tag{1}$$

where $n$ is the AWGN. Noisy and noiseless patches centered at a pixel $i \in N$ (the spatial domain) are extracted from $y$ or $x$, respec-

This research is supported in part by the 973 Program of China (No. 2012CB315803), the National Natural Science Foundation of China (Nos. 61371078, 61375054), and the Research Fund for the Doctoral Program of Higher Education of China (No. 20130002110051).

tively, as

$$y_i(u) = y(u+i), \quad x_i(u) = x(u+i), \quad u \in U$$

where $U$ is a neighborhood of the origin. Apply a wavelet transform to (1) , then (1) can be formulated as

$$Y_j = X_j + N_j \ \ (j \in 1, \cdots, M) \tag{2}$$

where $Y_j$, $X_j$ and $N_j$ are all scalar, representing the *j-th* wavelet coefficient of the noisy image $y$, noiseless image $x$, and noise $n$ at the same decomposition level, respectively; $M$ is the total number of wavelet coefficients, and (2) is obtained due to the linearity of the wavelet transform. Due to the orthonormality of the wavelet transform, $N_j$ is AWGN. Choosing LAWML to process the wavelet coefficients is mainly because of its simplicity and efficiency. LAWML then operates in two steps. The first step is to perform an approximate maximum *a posteriori* estimation of the variance $\sigma_j^2$ for each wavelet coefficient, which can use the coefficients of noisy image in a local neighborhood and a model for $\sigma_j^2$. The second step is to substitute $\sigma_j^2$ in the expression of minimum mean-squared error (MMSE) estimator of $X_j$. The expression of MMSE estimator $\hat{X}_j$ of $X_j$ is as follows

$$\hat{X}_j = \frac{\sigma_j^2}{\sigma_j^2 + \sigma_n^2} Y_j \tag{3}$$

where $\sigma_j^2$ is unknown. Hence, we can estimate $\sigma_j^2$ using a square window $R(j)$ where its center coefficient is at $Y_j$.

$$\begin{aligned} \hat{\sigma}_j^2 &= \underset{\sigma^2 \geq 0}{\arg\max} \prod_{i \in R(j)} P(Y_i | \sigma_i^2) \\ &= \max\left(0, \frac{1}{M} \sum_{i \in R(j)} Y_i^2 - \sigma_n^2\right) \end{aligned} \tag{4}$$

where $P(\cdot|\sigma^2)$ is the Gaussian distribution with zero mean and variance $\sigma^2 + \sigma_n^2$, and $M$ is the number of coefficients in the square window $R(j)$ centered at $Y_j$. After obtaining the estimator $\hat{\sigma}_j$ of $\sigma_j$, use $\hat{\sigma}_j^2$ instead of $\sigma_j^2$ in (3). In this case, $\sigma_n^2$ is also unknown in (3). An effective estimator for $\sigma_n$ is the median of absolute deviation using the finest scale wavelet coefficients [16].

$$\hat{\sigma}_n = \frac{median(|Y_j|)}{0.6745} \quad (Y_j \in \ subband\ HH) \tag{5}$$

### 2.2. NonLocal Means

The goal of denoising methods is to provide an estimation $\hat{x}$ of the clean image $x$. The denoised image $\hat{y}$ of the basic NL-means [12] lies in a weighted average of potential all the image pixels, i.e.

$$\hat{x}(i) = \sum_{j \in N} w(i,j) y(j), \quad i \in N \tag{6}$$

where $N$ is a regular pixel grid (the spatial domain), $w(i,j)_{j \in N}$ is the set of weights that characterize the pixel $i$, which sum to one. Each weight is determined by the patch similarity between patch $y_i$ and patch $y_j$, as

$$w(i,j) = e^{-\frac{d(i,j)}{h^2}} / \sum_{n \in N} e^{-\frac{d(i,n)}{h^2}} \tag{7}$$

where $d(i,j)$ is distance measure between patch $y_i$ and patch $y_j$; $h > 0$ is a parameter that controls the decay of the exponential function.

The distance $d$ is generally defined as a windowed quadratic distance between patches,i.e.

$$d(i,j) = \left|\left| y_i\sqrt{k} - y_j\sqrt{k} \right|\right|_2^2 \tag{8}$$

where $k$ is a windowing kernel. Typically, $k$ is rotational symmetric and the weights $k(u)$ are determined by the spatial distance from the center.

In this paper, we use *foveated distance* as distance measure, mainly due to the phenomenon, termed *foveated vision* described in the Foveated NL-means [17]. The *foveated distance*,i.e.

$$d^{FOV}(i,j) = ||\mathcal{F}[y,i] - \mathcal{F}[y,j]||_2^2 = \left|\left| y_i^{FOV} - y_j^{FOV} \right|\right|_2^2 \tag{9}$$

where $\mathcal{F}$ is a foveation operator, which corresponds to a spatially variant blurring operator with increasing blur at pixels far from the center. Thus, the NL-means enforces the patches similarity of natural images and turns out to be effective methods to remove the noise.

## 3. THE PROPOSED ALGORITHM

### 3.1. Multiscale Products

Signal singularities evolve across scales while noise decays rapidly along scales. Hence, we can imagine that multiplying the adjacent wavelet subbands would enhance edge structures while diluting noise. This favorite property has been exploited in [8, 18], etc. In this paper, we define the multiscale products of subbands of the noisy image as

$$P^z Y_j(k) = Y_j^z(k) \cdot Y_j^z(k+1) \quad (z = h, v, d) \tag{10}$$

where $k$ is the decomposition level of the corresponding subband, and $j$ is the position of coefficients in the corresponding subband; $h$, $v$ and $d$ represent the $horizontal$, $vertical$, and $diagonal$ direction subbands, respectively.

### 3.2. Incorporating Neighboring Coefficients in Multiscale Products

Wavelet coefficients are highly correlated in a small neighborhood, which implies that a large wavelet coefficient will likely have large coefficients at its neighbors, which is known as the intrascale dependencies. Hence, incorporating neighboring coefficients in the multiscale products instead of in the wavelet coefficients can combine the intrascale and interscale dependencies together.

For image denoising, an undecimated wavelet transform over $J$ stages is applied. At every decomposition level, three high-frequency subbands are derived. By calculating the energy of a neighboring area in the multiscale products, we can get more information of edges or structural information of the signals. A square window $R(j)$ is used for each product coefficient to compute the energy :

$$S_j^z(k) = \frac{1}{R^2} \sum_{m \in R(j)} [P_m^z Y_m^z(k)]^2 \tag{11}$$

where the window size $R$ should be $3 \times 3, 5 \times 5$, etc. We extend the work of edge dectection to the product coefficients like in [8] instead of the wavelet coefficients. A proper product threshold $\lambda$ can be determined as follows

$$\lambda = c \cdot \sigma^2(k) \cdot \log(R^2) \tag{12}$$

where $c$ is a variable parameter with $c = (0.2 \sim 0.3) \cdot \sigma_n$ (this is found empirically to perform well). Choosing a proper $c$ is a trade-off between preserving features and removing noise. Then the following rule is adopted in the thresholding process to identify the significant structures :

$$\hat{X}_j^z(k) = \begin{cases} \frac{\sigma_j^2}{\sigma_j^2+\sigma_n^2} Y_j^z(k) & \text{if } S_j^z(k) \geq \lambda \\ 0 & \text{otherwise} \end{cases} \quad (13)$$
$$(k = 1, \cdots, J-1; z = h, v, d)$$

$k$ is the decomposition level, and $z$=$h$, $v$, $d$ represents $horizontal$, $vertical$, $diagonal$ direction product subbands, respectively. $\sigma(k)$ in (12) is the standard deviation in the $k$th decomposition level of $diagonal$ product subband. Then, we use the median of absolute deviation of the $diagonal$ product subband to estimate $\sigma(k)$.

The proposed method mainly undergoes two stages shown in figure 1, which describes the diagram of the proposed method. 1 and 2 in the diagram means the start of the first and second stage of denoising, respectively. $y$, $WT$ and $MP$ represents noisy image, wavelet transform and multiscale products, respectively. $\hat{y}^w$ and $\hat{y}^n$ is the initial denoised image by the multiscale products and NL-means method, respectively. Thus the final denoised image can be as follows:

$$\hat{y} = w_1 \cdot \hat{y}^w + w_2 \cdot \hat{y}^n, \quad w_1 + w_2 = 1 \quad (14)$$

where $w_1$ and $w_2$ is the weights, which controls the significance of the initial denoised image by the multiscale products and NL-means methods. The proposed method can be summarized in Algorithm 1 .

**Algorithm 1** The Proposed *PMPA* Algorithm

1. In the first stage:
   1) Use the UWT to decompose the noisy image $y$ into $J$ scales and estimate the noise variance $\sigma_n^2$ of the noisy image using (5);
   2) Obtain the multiscale products using (10);
   3) For each product subband:
      a) Estimate the noise variance $\hat{\sigma}^2(k)$;
      b) Compute the product threshold $\lambda$ using (12);
      c) For each product coefficient:
         A) Compute the energy $S_j^z(k)$ using (11);
         B) Process the wavelet coefficients using (13);
   4) Obtain one initial denoised image $\hat{y}^w$ by inversing the wavelet transform.
2. In the second stage:
   (a) Obtain another initial denoised image $\hat{y}^n$ by performing NL-means in smooth regions (corresponding to small thresholding);
3. Obtain the final denoised image using (14).

## 4. EXPERIMENTAL RESULTS

We have taken various experiments to test the performance of our proposed method. An orthonormal wavelet basis with eight vanishing moments (sym8) over four levels of decomposition stages is

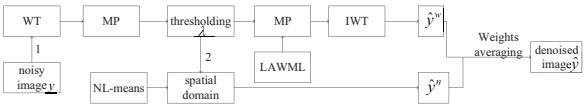


**Fig. 1**. Diagram of the proposed denoising method

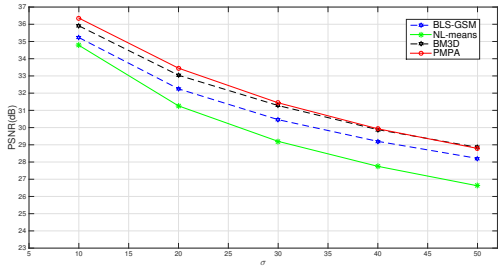


(a) PSNR

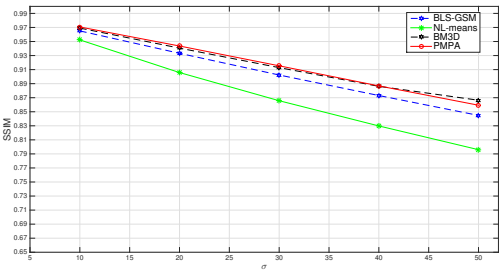


(b) SSIM

**Fig. 2**. Comparison with different methods for Lena. (a)Comparison in PSNR with Lena. (b)Comparison in SSIM with Lena.

applied and the window size $5 \times 5$ of LAWML is chosen empirically. For computational purposes of the NL-means method, we have fixed a search window of $10 \times 10$ pixels and a similarity square neighborhood of $5 \times 5$ in all the experiments of NL-means method; the value of $w_1$ is chosen empirically by 0.5. Further, we choose the most representative of the three state-of-the-art denoising methods, *BLS-GSM* [6], NL-means [12] and BM3D [13], as our benchmark. The other parameters of each denoising algorithm are consistent with the given values in the corresponding referred papers [6, 12, 13, 15]. We use Peak Signal to Noise Ration (PSNR) and the structural similarity (SSIM) index to evaluate performance of the denoising algorithms. For reliable comparisons, a number of standard grayscale images are used to test our algorithms, but only report results for *Lena*($512 \times 512$), *Barbara* ($512 \times 512$), *Peppers* ($512 \times 512$). *Barbara* and *Peppers* is the representative of the textured and smooth images, respectively. Every one is contaminated with additive white Gaussian noise at five different power levels $\sigma \in [10, 20, 30, 40, 50]$.

Table 1 summarizes the results obtained, and the best results are shown in boldface. As shown in Table 1, the PSNR values increases of 0.92 dB, 1.02 dB and 0.20 dB on average over BLS-GSM, NL-means and BM3D for *Lena*. The proposed PMPA can achieve better results for those images containing less textures, such as *Lena* and *Peppers*, but achieve a slightly worse results for those images containing lots of textures, such as *Barbara*, at different noise levels.

(a) Original image

(b) Noisy image (PSNR=18.61)

(c) BLS-GSM (PSNR=30.46)

(d) NL-means (PSNR=29.20)

(e) BM3D (PSNR=31.28)

(f) PMPA (PSNR=31.44)

**Fig. 3**. Example of the denoising results for Lena with $\sigma = 30$.

Figure 2 shows that the PSNR gains of the proposed PMPA method relative to NL-means is up to 2.1dB for *Lena* at $\sigma = 50$. Performance of the PMPA method is a slightly inferior to that of BM3D for Barbara, mainly due to the fact that BM3D is more appropriate for textured images and the search window size of NL-means is restricted to a small size. Thus the performance of PMPA can be further improved by enlarging the search window size, however, at the cost of computational cost, so we limit the search window size to a fixed value, which is a trade-off between the performance and computational complexity. Thus PMPA is more suitable for piecewise smooth images due to the property of NL-means.

The human eye is the only one to decide whether the quality of the images has been improved by the denoising algorithm. We display some denoising results comparing the PMPA with other state-of-the-art denoising methods in Figure 3. From Figure 3, we can realize that the proposed PMPA have better visual effects than BLS-GSM and NL-means, which have more ringing artifacts and less obvious edges, respectively. Compared with BM3D, both methods can remove most of noise effectively, however, the PMPA can have better visual effects in smooth zones.

As for the time complexity, the proposed denoising algorithm is similar to BM3D, higher than BLS-GSM and NL-means. The proposed method and BM3D get better results by sacrificing some amount of computation time to obtain better performances. However, the advantage of the proposed method is that it can obtain competitive performance compared with state-of-the-art denoising methods using a simple statistical model based on the multiscale products. The strategy of thresholding in the multiscale products can be used as a framework extended to many redundant transforms, such as nonsubsampled Contourlet transform (NSCT) [19] and Nonsubsampled Shearlet transform(NSST) [20], and so on, which can more effectively capture image edges and contours than UWT, to further improve the denoising performance.

**Table 1**. Summary of PSNR(dB) and SSIM index

| Lena | | | | | | |
|---|---|---|---|---|---|---|
| $\sigma_n$ | 10 | 20 | 30 | 40 | 50 | Average |
| BLS-GSM | 35.230<br>0.9651 | 32.25<br>0.9332 | 30.46<br>0.9023 | 29.20<br>0.8731 | 28.21<br>0.8448 | 31.07<br>0.9037 |
| NL-means | 34.78<br>0.9523 | 31.26<br>0.9058 | 29.20<br>0.8657 | 27.75<br>0.8298 | 26.62<br>0.7960 | 29.92<br>0.8699 |
| BM3D | 35.91<br>0.9691 | 33.04<br>0.9406 | 31.28<br>0.9128 | 29.88<br>0.8862 | **28.85**<br>**0.8664** | 31.79<br>0.9150 |
| PMPA | **36.36**<br>**0.9707** | **33.45**<br>**0.9436** | **31.44**<br>**0.9154** | **29.93**<br>**0.8868** | 28.79<br>0.8593 | **31.99**<br>**0.9152** |
| Barbara | | | | | | |
| BLS-GSM | 33.13<br>0.9681 | 29.08<br>0.9230 | 26.79<br>0.8753 | 25.30<br>0.8312 | 24.33<br>0.7930 | 27.73<br>0.8781 |
| NL-means | 33.70<br>0.9661 | 29.79<br>0.9169 | 27.18<br>0.8643 | 25.44<br>0.8138 | 24.22<br>0.7674 | 28.07<br>0.8657 |
| BM3D | **34.93**<br>**0.9767** | **31.71**<br>**0.9524** | **29.73**<br>**0.9250** | **27.95**<br>**0.8921** | **27.15**<br>**0.8686** | **30.29**<br>**0.9230** |
| PMPA | 34.79<br>0.9755 | 30.36<br>0.9371 | 27.51<br>0.8891 | 25.76<br>0.8439 | 24.74<br>0.8069 | 28.63<br>0.8905 |
| Peppers | | | | | | |
| BLS-GSM | 34.53<br>0.9641 | 32.02<br>0.9365 | 30.39<br>0.9094 | 29.13<br>0.8821 | 28.13<br>0.8563 | 30.84<br>0.9097 |
| NL-means | 34.12<br>0.9546 | 31.43<br>0.9197 | 29.58<br>0.8898 | 29.20<br>0.8618 | 26.86<br>0.8337 | 30.24<br>0.8919 |
| BM3D | 34.99<br>0.9658 | 32.71<br>0.9413 | 31.16<br>0.9178 | 29.85<br>0.8947 | 28.75<br>0.8791 | 31.49<br>0.9197 |
| PMPA | **35.34**<br>**0.9683** | **33.12**<br>**0.9474** | **31.48**<br>**0.9261** | **29.93**<br>**0.8968** | **28.95**<br>**0.8826** | **31.76**<br>**0.9242** |

## 5. CONCLUSIONS

In this paper, we have proposed a new patch-based multiscale products algorithm (PMPA), combining the patch similarity in spatial domain and the intra-interscale dependencies in wavelet domain. Noisy images are processed by NL-means in spatial domain and multiscale products method in wavelet domain, respectively, and then obtain the final denoised image. Experimental results show that the proposed PMPA can achieve competitive performance and have better visual effects compared with other state-of-the-art patch-based denoising methods. It should be mentioned that the search window size of NL-means is restricted to a small value. Hence, the performance of PMPA can be further improved by enlarging the search window size in the noisy images.

## 6. REFERENCES


[1] L. Shao, R. Yan, X. Li, and Y. Liu, "From heuristic optimization to dictionary learning: A review and comprehensive comparison of image denoising algorithms," *Cybernetics, IEEE Transactions on*, vol. 44, no. 7, pp. 1001–1013, July 2014.

[2] H. Rabbani and S. Gazor, "Image denoising employing local mixture models in sparse domains," *Image Processing, IET*, vol. 4, no. 5, pp. 413–428, October 2010.

[3] F. Yan, L. Cheng, and S. Peng, "A new interscale and intrascale orthonormal wavelet thresholding for sure-based image denoising," *Signal Processing Letters, IEEE*, vol. 15, pp. 139–142, 2008.

[4] G. Chen, T. Bui, and A. Krzyzak, "Image denoising using neighbouring wavelet coefficients," in *Acoustics, Speech, and Signal Processing, 2004. (ICASSP '04). IEEE International Conference on*, vol. 2, May 2004, pp. ii–917–20 vol.2.

[5] F. Luisier, T. Blu, and M. Unser, "A new sure approach to image denoising: Interscale orthonormal wavelet thresholding," *Image Processing, IEEE Transactions on*, vol. 16, no. 3, pp. 593–606, March 2007.

[6] J. Portilla, V. Strela, M. Wainwright, and E. Simoncelli, "Image denoising using scale mixtures of gaussians in the wavelet domain," *Image Processing, IEEE Transactions on*, vol. 12, no. 11, pp. 1338–1351, Nov. 2003.

[7] L. Sendur and I. Selesnick, "Bivariate shrinkage functions for wavelet-based denoising exploiting interscale dependency," *Signal Processing, IEEE Transactions on*, vol. 50, no. 11, pp. 2744–2756, Nov. 2002.

[8] P. Bao and D. Zhang, "Noise reduction for magnetic resonance images via adaptive multiscale products thresholding," *Medical Imaging, IEEE Transactions on*, vol. 22, no. 9, pp. 1089–1099, Sept. 2003.

[9] K. Gupta and R. Gupta, "Feature adaptive wavelet shrinkage for image denoising," in *Signal Processing, Communications and Networking, 2007. ICSCN '07. International Conference on*, Feb. 2007, pp. 81–85.

[10] T. T. Cai and B. W. Silverman, "Incorporating information on neighbouring coefficients into wavelet estimation," *Sankhy: The Indian Journal of Statistics, Series B (1960-2002)*, vol. 63, no. 2, pp. pp. 127–148, 2001.

[11] L. Sendur and I. Selesnick, "Bivariate shrinkage with local variance estimation," *Signal Processing Letters, IEEE*, vol. 9, no. 12, pp. 438–441, Dec. 2002.

[12] A. Buades, B. Coll, and J.-M. Morel, "A non-local algorithm for image denoising," in *Computer Vision and Pattern Recognition, 2005. CVPR 2005. IEEE Computer Society Conference on*, vol. 2, June 2005, pp. 60–65 vol. 2.

[13] K. Dabov, A. Foi, V. Katkovnik, and K. Egiazarian, "Image denoising by sparse 3-d transform-domain collaborative filtering," *Image Processing, IEEE Transactions on*, vol. 16, no. 8, pp. 2080–2095, Aug 2007.

[14] J. Mairal, F. Bach, J. Ponce, G. Sapiro, and A. Zisserman, "Non-local sparse models for image restoration," in *Computer Vision, 2009 IEEE 12th International Conference on*, Sept 2009, pp. 2272–2279.

[15] M. Kivanc Mihcak, I. Kozintsev, K. Ramchandran, and P. Moulin, "Low-complexity image denoising based on statistical modeling of wavelet coefficients," *Signal Processing Letters, IEEE*, vol. 6, no. 12, pp. 300–303, Dec. 1999.

[16] D. L. Donoho and J. M. Johnstone, "Ideal spatial adaptation by wavelet shrinkage," *Biometrika*, vol. 81, no. 3, pp. 425–455, 1994.

[17] A. Foi and G. Boracchi, "Anisotropically foveated nonlocal image denoising," in *Image Processing (ICIP), 2013 20th IEEE International Conference on*, Sept 2013, pp. 464–468.

[18] M. Vijay, S. Subha, and K. Karthik, "Adaptive spatial and wavelet multiscale products thresholding method for medical image denoising," in *Computing, Electronics and Electrical Technologies (ICCEET), 2012 International Conference on*, March 2012, pp. 1109–1114.

[19] A. da Cunha, J. Zhou, and M. Do, "The nonsubsampled contourlet transform: Theory, design, and applications," *Image Processing, IEEE Transactions on*, vol. 15, no. 10, pp. 3089–3101, Oct. 2006.

[20] G. Easley, D. Labate, and W.-Q. Lim, "Sparse directional image representations using the discrete shearlet transform," *Applied and Computational Harmonic Analysis*, vol. 25, no. 1, pp. 25 – 46, 2008.